SF2A 2009
M. Heydari-Malayeri, C. Reylé and R. Samadi (eds)

PRIMORDIAL NON-GAUSSIANITY IN THE HALO BIAS

Desjacques, V.[1]

Abstract. Primordial non-Gaussianity of the local type induces a scale-dependent bias in the clustering of rare objects. Calibration with numerical simulations is essential to measurements of galaxy/quasar power spectra that aim to put constraint on the amount of primordial non-Gaussianity. We compare theoretical predictions with the outcome of large N-body simulations evolved from Gaussian and non-Gaussian initial conditions. At low wavenumber $k < 0.03\ h\mathrm{Mpc}^{-1}$, the theory and the simulations agree well with each other for haloes with linear bias $b(M) > 1.5$. Including a scale-independent bias correction improves the comparison between theory and simulations on smaller scales where the k-dependent effect becomes rapidly negligible. We place limits on the size of the cubic order correction using a compilation of large-scale structures data.

1 Introduction

A wide class of inflationary scenarios lead to non-Gaussianity of the local type, i.e. which depends on the local value of the primordial curvature perturbation (Here and henceforth, the usual Bardeen potential in matter-dominated era). In these models, deviation from Gaussianity can be conveniently parametrised by the nonlinear coupling parameters f_{NL} and g_{NL} through the relation

$$\Phi(\mathbf{x}) = \phi(\mathbf{x}) + f_{\mathrm{NL}}\phi(\mathbf{x})^2 + g_{\mathrm{NL}}\phi(\mathbf{x})^3 , \tag{1.1}$$

where $\phi(\mathbf{x})$ is an isotropic Gaussian random field whose power spectrum is a power-law $P_\phi(k) \sim k^{n_s-4}$. Note that the quadratic correction is small since curvature perturbations are typically $\mathcal{O}(10^{-5})$.

The cosmic microwave background (CMB) and large scale structures offer two different routes to test for the presence of primordial non-Gaussianity. The main advantage of the CMB resides in the fact that the observed spherical harmonics coefficient a_l^m are a linear superposition of the primordial curvature perturbations (weighted by the radiation transfer function). Therefore, any non-zero three-point and/or higher correlation function of $\Phi(\mathbf{x})$ is directly mirrored in the corresponding statistics of the primary temperature anisotropies. Thus far, analysis of the CMB three-point function indicates that the data is fully consistent with Gaussianity, with $-9 < f_{\mathrm{NL}} < +111$ at 95% C.L. (Komatsu et al. 2009).

Unlike the CMB, nonlinear gravitational evolution of large-scale structures can significantly contaminate the signal due to primordial non-Gaussianity. However, causality implies that this contamination decays rapidly as one goes to large distances. Another important difference with the CMB is that large-scale structures are traced by galaxies etc. which are biased relative to the matter distribution (since these preferentially form in overdense regions). As a consequence of this bias relation, high order statistics of the matter density field (such as the three-point function) can project onto low order statistics of biased tracers (such as the power spectrum). In particular, Dalal et al. (2008), Matarrese & Verde (2008), Slosar et al. (2008), showed that the three-point function for the local quadratic coupling $f_{\mathrm{NL}}\phi^2$ induces a scale-dependent bias $\Delta b_\kappa(k, f_{\mathrm{NL}})$ in the large-scale power spectrum of biased tracers,

$$\Delta b_\kappa(k, f_{\mathrm{NL}}) = 3f_{\mathrm{NL}}\left[b(M)-1\right]\delta_{\mathrm{c}}\frac{\Omega_{\mathrm{m}}H_0^2}{k^2T(k)D(z)} , \tag{1.2}$$

[1] Institute for Theoretical Physics, University of Zürich, Winterthurerstrasse 190, CH-8057 Zürich, Switzerland

where $b(M)$ is the linear bias parameter, H_0 is the Hubble parameter, $T(k)$ is the matter transfer function normalised to unity as $k \to 0$, $D(z)$ is the growth factor normalised to $(1+z)^{-1}$ in the matter era and $\delta_c \sim 1.68$ is the present-day (linear) critical density threshold. Slosar et al. (2008) applied this relation to constrain the value of $f_{\rm NL}$ using a compilation of large-scale structures data and found limits comparable to those from WMAP5, $-29 < f_{\rm NL} < +69$. Still, in order to fully exploit the potential of forthcoming galaxy surveys, theoretical predictions for the non-Gaussian bias need to be tested against the outcome of large numerical simulations. Here we study the impact of local non-Gaussianity on the bias of dark matter haloes.

2 N-body simulations

Investigating the scale-dependence of the halo bias requires simulations large enough so that many long wavelength modes are sampled. At the same time, the simulations should resolve the dark matter haloes hosting the surveyed objects, i.e. luminous red galaxies (LRGs) or quasars (QSOs), so that one can construct halo samples whose statistical properties mimic as closely as possible those of the real data.

We utilise a series of large N-body (collisionless) simulations of the ΛCDM cosmology seeded with Gaussian and non-Gaussian initial conditions. We adopt the standard (CMB) convention in which the Bardeen potential $\Phi(\mathbf{x})$ is primordial, and not extrapolated to present epoch. We run five sets of three 1024^3 simulations, each of which has $f_{\rm NL} = 0, \pm 100$, with the N-body code GADGET-2 (Springel 2005). We use the same Gaussian random seed field ϕ in each set of runs so as to minimise the sampling variance. The box size is 1600 h^{-1}Mpc such that the particle mass of these simulations is 3.0×10^{11} $\mathrm{M}_\odot/h$, enough to resolve haloes down to 10^{13} $\mathrm{M}_\odot/h$. Dark matter haloes are identified using the MPI parallelised version of the AHF halo finder which is based on the spherical overdensity (SO) finder developed by Gill, Knebe & Gibson (2004).

We interpolate the dark matter particles and halo centres onto a regular cubical mesh. The resulting dark matter and halo fluctuation fields were then Fourier transformed to yield the matter-matter, halo-matter and halo-halo power spectra $P_{\rm mm}(k)$, $P_{\rm mh}(k)$ and $P_{\rm hh}(k)$, respectively. These power spectra are measured for various halo masses and redshifts, covering a range of statistical properties corresponding to those of the available galaxy or quasar populations with different luminosities and bias. Note that these quantities are computed on a 512^3 grid, whose Nyquist wavenumber is sufficiently large (≈ 1 hMpc^{-1}) to allow for an accurate measurement of the power in wavemodes of amplitude $k \lesssim 0.1$ hMpc^{-1}. The halo power spectrum is corrected for the shot-noise due to the discrete nature of dark matter haloes, which we assume to be the standard Poisson term $1/\bar{n}$. Yet another important quantity is the linear halo bias $b(M)$ which must be measured accurately from the Gaussian simulations as it controls the magnitude of the scale-dependent shift (see equation 1.2). We use the ratio $P_{\rm mh}(k)/P_{\rm mm}(k)$ as a proxy for the halo bias since it is less sensitive to shot-noise.

In order to quantify the effect of non-Gaussianity on the halo bias, we consider the ratios

$$\begin{aligned} \frac{P_{\rm mh}(k,f_{\rm NL})}{P_{\rm mh}(k,0)} - 1 &= \frac{\Delta b(k,f_{\rm NL})}{b(M)} \\ \frac{P_{\rm hh}(k,f_{\rm NL})}{P_{\rm hh}(k,0)} - 1 &= \left(1 + \frac{\Delta b(k,f_{\rm NL})}{b(M)}\right)^2 - 1\,. \end{aligned} \tag{2.1}$$

Although $P_{\rm mh}$ is less affected by discreteness, it is important to measure the effect in the auto-power spectrum $P_{\rm hh}$ of dark matter haloes since the latter gives the strongest constraint on $f_{\rm NL}$.

3 Non-Gaussian bias shift

At the lowest order, there are two additional, albeit relatively smaller, corrections to the halo bias which arise from the dependence of both the halo number density $n(M,z)$ and the matter power spectrum $P_{\rm mm}$ on the nonlinear parameter $f_{\rm NL}$. These terms must be included in the comparison with the simulations (Desjacques, Seljak & Iliev 2009).

Firstly, assuming the peak-background split holds, the change in the mean number density of haloes induces a k-independent shift

$$\Delta b_{\rm I}(f_{\rm NL}) = -\frac{1}{\sigma}\frac{\partial}{\partial \nu}\ln\left[R(\nu, f_{\rm NL})\right] \tag{3.1}$$

where $\nu = \delta_c(z)/\sigma(M)$ is the peak height at mass scale M and $R(\nu, f_{NL})$ is the fractional correction to the Gaussian mass function. Notice that $\Delta b_I(f_{NL})$ has a sign opposite to that of f_{NL}, because the bias decreases when the mass function goes up (cf. left panel of Fig. 1).

Secondly, primordial non-Gaussianity affects the matter power spectrum as positive values of f_{NL} tend to increase the small-scale power. For $f_{NL} \sim \mathcal{O}(10^2)$, the magnitude of this correction is at a per cent level in the weakly nonlinear regime $k \lesssim 0.1\ h\mathrm{Mpc}^{-1}$. We find that leading order perturbation theory (PT) provides an excellent description of the effect over the wavenumbers of interest, $k \lesssim 0.1\ h\mathrm{Mpc}^{-1}$ (cf. left panel of Fig. 1).

Summarising, local non-Gaussianity adds a correction $\Delta b(k, f_{NL})$ to the bias $b(k)$ of dark matter haloes that can be written as

$$\Delta b(k, f_{NL}) = \Delta b_\kappa(k, f_{NL}) + \Delta b_I(f_{NL}) + b(M)\beta_m(k, f_{NL}) \tag{3.2}$$

at first order in f_{NL}, where $\beta_m(k, f_{NL}) = P_{mm}(k, f_{NL})/P_{mm}(k, 0) - 1$. The right panel of Fig. 1 illustrates the relative contribution of these terms for haloes of mass $M > 2 \times 10^{13}\ \mathrm{M}_\odot/h$ identified at redshift $z = 0.5$. The data points are obtained from measurements of the cross-power spectrum in the N-body simulations. The solid curve shows the total non-Gaussian bias $\Delta b(k, f_{NL})$. Considering only the scale-dependent shift Δb_κ leads to an apparent suppression of the effect in simulations relative to the theory. Including the scale-independent correction Δb_I considerably improves the agreement at wavenumbers $k \lesssim 0.05\ h\mathrm{Mpc}^{-1}$. Finally, adding the scale-dependent term $b(M)\beta_m$ further adjusts the match at small scale $k \gtrsim 0.05\ h\mathrm{Mpc}^{-1}$ by making the non-Gaussian bias shift less negative.

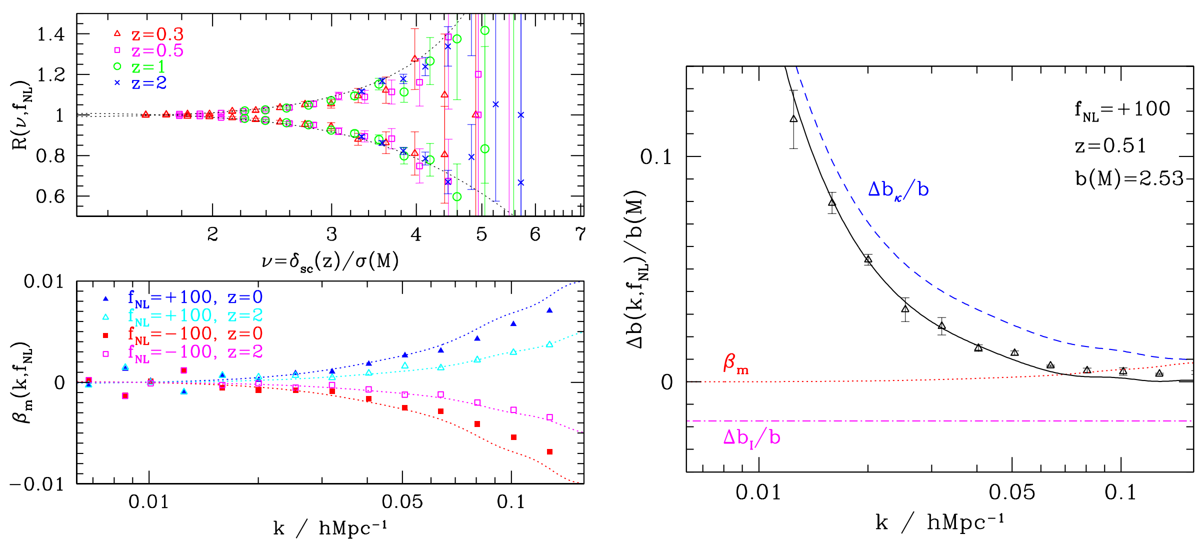

Fig. 1. Upper left: Fractional deviation from the fiducial Gaussian mass function. Different symbols refer to different redshifts as indicated. Error bars denote Poisson errors. **Lower Left**: Non-Gaussian fractional correction to the matter power spectrum, $\beta_m(k, f_{NL}) = P_{mm}(k, f_{NL})/P_{mm}(k, 0) - 1$, that originates from primordial non-Gaussianity of the local type. Results are shown at redshift $z = 0$ and 2 for $f_{NL} = \pm 100$. The dotted curves indicate the prediction from a leading-order perturbative expansion. **Right**: Non-Gaussian bias correction for haloes of mass $M > 2 \times 10^{13}\ \mathrm{M}_\odot/h$ extracted from the snapshot at $z = 0.5$ (filled symbols). The solid curve represents our theoretical model eq. (3.2). The dashed, dotted-dashed-dotted and dotted curves show the three separate contributions that arise at first order in f_{NL}. Our theoretical scaling agrees very well with the data for $k \lesssim 0.05\ h\mathrm{Mpc}^{-1}$.

If haloes and dark matter do not trace each other on large scales, i.e. if there is stochasticity, then analyses based on the auto- and cross-power spectrum may not agree with each other. While models with Gaussian initial conditions predict little stochasticity on large scales, this has not been shown explicitly for models with non-Gaussianity. We find that measurements of the non-Gaussian bias correction obtained with the halo-halo or the halo-matter power spectrum are in a good agreement with each other, suggesting that non-Gaussianity does not induce stochasticity and the predicted scaling applies equally well for the auto- and cross-power spectrum.

For highly biased haloes ($b(M) \gtrsim 1.5$), our results indicate that the simulated non-Gaussian bias converges towards the theoretical prediction for $k \lesssim 0.03\ h\mathrm{Mpc}^{-1}$. At smaller scales, the effect depends strongly on scale-independent bias. If we include this contribution using analytic calculation (equation 3.1), the suppression relative to theory is much smaller and in some cases goes in the opposite direction. Still, one could argue that scale-independent bias cannot be identified from the data alone, so one should fit for it and include it in the overall bias, as was done in Slosar et al. (2008). In this case the agreement between theory and simulations is improved further. For the halo samples with $b(M) \lesssim 1.5$ there is some evidence that the actual bias exceeds the theory on all scales. Therefore, the proposed eq. (3.2) does not appear to be universal, so care must be exercised when applied to the actual large scale structure data.

4 Constraints on $g_{\rm NL}$ (trispectrum)

Thus far, we have only considered the effect of the quadratic term $f_{\rm NL}\phi^2$ on the clustering of dark matter haloes. However, in inflationary scenarios such as the curvaton model, a large cubic correction $g_{\rm NL}\phi^3$ can be produced while simultaneously keeping the quadratic correction small. Therefore, we have also explored the effect of the cubic term on the halo bias (Desjacques & Seljak 2009). Simulations of non-Gaussian models with $g_{\rm NL} = \pm 10^6$ and with properties similar to those of the aforementioned simulations are used to calibrate the theory. The k-dependence of the bias correction $\Delta b_\kappa(k, g_{\rm NL})$ measured from the auto- and cross-power spectrum of haloes, is similar to that found in $f_{\rm NL}$ models, but the amplitude is lower than theoretical expectations. Using the compilation of large-scale structure data of Slosar et al. (2008), we obtain for the first time a limit on $g_{\rm NL}$ of

$$-3.5 \times 10^5 < g_{\rm NL} < +8.2 \times 10^5 \quad \text{(at 95\% CL)} \tag{4.1}$$

For the limits obtained here, $\Delta b_{\rm I}$ should be much smaller than $b(M)$ and can thus be ignored. Note also that, whereas the non-Gaussian bias scales as $D(z)^{-1}$ in $f_{\rm NL}$ models, the redshift dependence is stronger for $g_{\rm NL}$ non-Gaussianity, $\Delta b(k, g_{\rm NL}) \propto D(z)^{-2}$, so one can achieve relatively larger gains from measurements of high redshift tracers. We expect our limit to improve by 1-2 orders of magnitude with future large-scale structures data. In fact, the extent to which one can tighten the observational bounds will mainly depend on our ability to minimise the impact of sampling variance caused by the random nature of the wavemodes, and the shot-noise caused by the discrete nature of the tracers. By comparing differently biased tracers of the same surveyed volume (Seljak 2009) and suitably weighting galaxies (Seljak, Hamaus, & Desjacques 2009), it should be possible to circumvent these problems and considerably improve the detection level.

References

Dalal, N., Doré, O., Huterer, D., & Shirokov, A., 2008, Phys. Rev. D, 77, 123514

Desjacques, V., Seljak, U., & Iliev, I.T., 2009, MNRAS, 396, 85

Desjacques, V., & Seljak, U., 2009, arXiv:0907.2257

Gill, S.P.D., Knebe, A., & Gibson, B.K., 2004, MNRAS, 351, 399

Komatsu, E., et al., 2009, ApJS, 180, 330

Matarrese, S., & Verde, L., 2008, ApJ, 677, L77

Seljak, U., 2009, Phys. Rev. Lett., 102, 021302

Seljak, U., Hamaus, N., & Desjacques, V., 2009, arXiv:0904.2963

Slosar, A., Hirata, C., Seljak, U., Ho, S., & Padmanabhan, N., 2008, JCAP, 8, 31

Springel, V., 2005, MNRAS, 364, 1105